

# Unexpected Structural Preference for Aggregates with Metallophilic Ag–Au Contacts in (Trimethylphosphine)silver(I) and -gold(I) Phenylethynyl Complexes. An Experimental and Theoretical Study

Oliver Schuster, Uwe Monkowius, Hubert Schmidbaur,\* R. Shyama Ray, Sven Krüger, and Notker Rösch\*

Department Chemie, Technische Universität München, Lichtenbergstrasse 4, 85747 Garching, Germany

Received November 16, 2005

(Me<sub>3</sub>P)AuC≡CPh is a molecular compound associated into chains through aurophilic contacts, while its silver analogue exists as the ionic isomer [(Me<sub>3</sub>P)<sub>2</sub>Ag]<sup>+</sup>[Ag(C≡CPh)<sub>2</sub>]<sup>−</sup>. Equivalent mixtures of the two compounds (Au:Ag = 1:1) in dichloromethane yield the ionic mixed-metal compound [(Me<sub>3</sub>P)<sub>2</sub>Ag]<sup>+</sup>[Au(C≡CPh)<sub>2</sub>]<sup>−</sup>, which is stable in solution only in the presence of an excess of the Me<sub>3</sub>P ligand. Under these conditions it can be crystallized, and in the crystals the cations and the anions (with idealized D<sub>3d</sub> and D<sub>2h</sub> symmetry, respectively) are aggregated via heterometallophilic bonding, generating linear –Ag–Au–Ag–Au– chains. The solid was found to be also unstable at room temperature, owing to a rapid loss of four out of six tertiary phosphines, which leads to a product of the composition [(Me<sub>3</sub>P)<sub>2</sub>Ag]<sup>+</sup>[Ag<sub>2</sub>Au<sub>3</sub>(C≡CPh)<sub>6</sub>]<sup>−</sup>. By crystal structure analysis, the anion was shown to have three [PhC≡CAuC≡CPh]<sup>−</sup> anions associated via two Ag<sup>+</sup> cations to give a Ag<sub>2</sub>Au<sub>3</sub> core unit of quasi-D<sub>3h</sub> symmetry. Structure and bonding in this anion have been analyzed through density functional calculations of the [Ag<sub>2</sub>Au<sub>3</sub>(C≡CH)<sub>6</sub>]<sup>−</sup> model and shown to be largely ionic in nature. Deviations of the experimental and calculated geometrical details could be traced to the electrostatic field in the crystal. In the unit cell, the cluster anions are associated with the [(Me<sub>3</sub>P)<sub>2</sub>Ag]<sup>+</sup> cations (of idealized D<sub>3h</sub> symmetry) via heterometallophilic contacts in which two of the three gold atoms are involved.

## Introduction

Most solid-state structures and many molecular configurations and conformations of two-coordinated gold(I) complexes are strongly influenced or even determined by aurophilic interactions.<sup>1–3</sup> The gain in energy resulting from an intra- or intermolecular mutual approach of two formally “closed-shell” gold centers is known to be on the order of 5–10 kcal/contact and thus is in the same range as for conventional hydrogen bonds.<sup>4</sup> This phenomenon has attracted considerable interest, and the number of reports on experimental observations and theoretical treatments has increased very rapidly because Au–Au interactions are associated with novel mesogenic, nonlinear optical, and in particular photoemissive properties of the molecules and their aggregates.<sup>5</sup>

Similar observations have also been made with related silver(I) compounds, and argentophilic interactions are considered in all recent, more detailed discussions of molecular and solid-state structures of silver(I) complexes.<sup>6–10</sup> Although the energy associated with Ag–Ag contacts (for which there are

only limited experimental data) appears to be lower than for Au–Au contacts, the effect may yet be significant in many condensed systems.<sup>11</sup>

In the past few years empirical evidence has finally also been accumulated for *mixed-metal Au–Ag interactions*, addressed very generally as metallophilic bonding between 5d<sup>10</sup> and 4d<sup>10</sup> centers.<sup>12–20</sup> In the course of our own recent studies of gold(I) and silver(I) ethynyl complexes we have become confronted with a few particularly striking examples of apparently metallophilicity-induced reaction patterns and structural motifs which were then followed up by complementary preparative experiments, structural studies, and theoretical calculations. One set

(1) Schmidbaur, H.; Cronje, S.; Djordjevic, B.; Schuster, O. *Chem. Phys.* **2005**, *311*, 151.

(2) Schmidbaur, H.; Grohmann, A.; Olmos, M. E. In *Gold: Progress in Chemistry, Biochemistry and Technology*; Schmidbaur, H., Ed.; Wiley: Chichester, U.K., 1999; p 647.

(3) Pyykkö, P. *Angew. Chem. Int. Ed.* **2004**, *43*, 441.

(4) Mingos, D. M. P. *J. Chem. Soc., Dalton Trans.* **1996**, *5*, 561.

(5) Parish, R. V. *Gold Bull.* **1998**, *1*, 14.

(6) Djordjevic, B.; Schuster, O.; Schmidbaur, H. *Inorg. Chem.* **2005**, *3*, 673.

(7) Fernandez, E. J.; Lopez-de-Luzuriaga, J. M.; Monge, M.; Rodriguez, M. A.; Crespo, O.; Gimeno, M. C.; Laguna, A.; Jones, P. G. *Inorg. Chem.* **1998**, *23*, 6002.

(8) El-Bahraoui, J.; Molina, J. M.; Olea, D. P. *J. Phys. Chem.* **1998**, *102*, 2443.

(9) Siemeling, U.; Vorfeld, U.; Neumann, B.; Stammler, H.-G. *J. Chem. Soc., Chem. Commun.* **1997**, 1723.

(10) Poblet, J.-M.; Benard, M. *J. Chem. Soc., Chem. Commun.* **1998**, 1179.

(11) Zhang, J.-P.; Wang, Y.-B.; Huang, X.-C.; Lin, Y.-Y.; Chen, X.-M. *Chem. Eur. J.* **2005**, *11*, 552.

(12) Usón, R.; Laguna, A.; Laguna, M.; Jones, P. G.; Sheldrick, G. M. *J. Chem. Soc., Chem. Commun.* **1981**, 1097.

(13) Usón, R.; Laguna, A.; Laguna, M.; Manzano, B. R.; Jones, P. G.; Sheldrick, G. M. *J. Chem. Soc., Dalton Trans.* **1984**, 285.

(14) Usón, R.; Laguna, A.; Laguna, M.; Manzano, B. R.; Tapia, A. *Inorg. Chim. Acta* **1985**, *101*, 151.

(15) Usón, R.; Laguna, A.; Laguna, M.; Uson, A.; Jones, P. G.; Freire Erdbrügger, C. *Organometallics* **1987**, *8*, 1778.

(16) Rawashdeh-Omary, M. A.; Omary, M. A.; Fackler, J. P. *Inorg. Chim. Acta* **2002**, *334*, 376.

(17) (a) Abu-Salah, O. M.; Knobler, C. B. *J. Organomet. Chem.* **1986**, *302*, C10. (b) Abu-Salah, U. M.; Al-Ohaly, A. R.; Knobler, C. B. *J. Chem. Soc., Chem. Commun.* **1985**, 1502.

(18) Mazhar Ul, H.; Horne, W.; Abu-Salah, O. M. *J. Crystallogr. Spectrosc. Res.* **1992**, *4*, 421.

(19) Hussain, M. S.; Ul-Haque, M.; Abu-Salah, O. M. *J. Cluster Sci.* **1996**, *2*, 167.

(20) Abu-Salah, O. M. *J. Organomet. Chem.* **1998**, *565*, 211 and references therein.

of results on phenylethynylgold(I) and -silver(I) complexes is summarized in the present account.

There is extensive literature on gold(I) and silver(I) ethynyls which has been reviewed several times in the secondary and tertiary literature,<sup>2,21–24</sup> and a comprehensive treatment is again in preparation. For background information, the reader is referred to these coverages. References of the most recent work<sup>25,26</sup> can also serve as key citations.

## Preparative Results

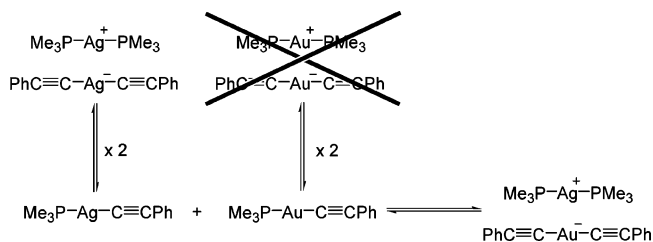
As described in an earlier account, (*trimethylphosphine*)-*phenylethynylgold(I)* is obtained from the reaction of equimolar quantities of  $(\text{Me}_3\text{P})\text{AuCl}$  and  $\text{LiC}\equiv\text{CPh}$  in THF at  $-78\text{ }^\circ\text{C}$ . The structure and spectroscopic properties have been reported.<sup>27</sup> In this context it should be emphasized that the NMR spectra of solutions of  $(\text{Me}_3\text{P})\text{AuC}\equiv\text{CPh}$  in dichloromethane are not temperature-dependent. The  $^1\text{H}$  and  $^{13}\text{C}$  resonances of the  $\text{PMe}_3$  ligands are clean first-order doublets, indicating that no ligand redistribution takes place in solution to give, for example, the homoleptic ions  $[(\text{Me}_3\text{P})_2\text{Au}]^+$  and  $[\text{Au}(\text{C}\equiv\text{CPh})_2]^-$ , the former of which would give rise to  $A_9XX'A'_9$  and  $AXX'$  spin systems, respectively.

*Phenylethynylsilver(I)* was first described by Glaser as early as 1870.<sup>28</sup> It is obtained as the brown, insoluble polymer  $[\text{AgC}\equiv\text{CPh}]_n$  from  $\text{PhC}\equiv\text{CH}$  and silver salts and has a variable analytical composition, depending on the reagents and reaction conditions. It can be dissolved in dichloromethane upon addition of a solution of an equimolar amount of  $\text{Me}_3\text{P}$  (in toluene), and the product crystallizes from dichloromethane/pentane (85% yield, mp  $173\text{ }^\circ\text{C}$  with decomposition). The temperature dependence of the NMR data collected in this work for solutions in dichloromethane suggests a dynamic behavior, the compound partly undergoing ligand redistribution to the homoleptic, ionic complex  $[(\text{Me}_3\text{P})_2\text{Ag}]^+[\text{Ag}(\text{C}\equiv\text{CPh})_2]^-$ . This result confirms an early crystal structure analysis by Corfield and Shearer.<sup>29</sup>

Surprisingly, the reaction of  $[(\text{Me}_3\text{P})_2\text{Ag}]^+[\text{Ag}(\text{C}\equiv\text{CPh})_2]^-$  with 2 equiv of  $(\text{Me}_3\text{P})\text{Au}(\text{C}\equiv\text{CPh})$  (ratio Ag:Au = 1:1) in dichloromethane at  $20\text{ }^\circ\text{C}$  was found to give crystalline products which have a variable composition depending on the reaction and workup times. It was only upon addition of an excess of free  $\text{Me}_3\text{P}$  to the reaction mixture that a crystalline product of the expected composition with a ratio  $\text{Me}_3\text{P}:\text{Ag}:\text{Au}:\text{C}\equiv\text{CPh} = 2:1:1:2$  could be isolated in high yield (87%). Upon heating this colorless crystalline solid melts with decomposition at  $153\text{--}155\text{ }^\circ\text{C}$ . However, the samples always are distinctly malodorous and appear to lose  $\text{Me}_3\text{P}$ .

By analytical, spectroscopic, and structural data it has been confirmed that the compound has the ionic structure  $[(\text{Me}_3\text{P})_2\text{Ag}]^+[\text{Au}(\text{C}\equiv\text{CPh})_2]^-$ . The NMR spectra of solutions in dichloromethane are again temperature dependent and

## Scheme 1



suggest the coexistence of homo- and heteroleptic species, as shown in Scheme 1. Even at  $-85\text{ }^\circ\text{C}$  no complete resolution can be achieved. For the solid (in KBr), the IR absorption for  $\nu(\text{C}\equiv\text{C})$  appears at  $2097\text{ cm}^{-1}$ , similar to the absorptions for the salts  $[\text{Ph}_3\text{PMe}]^+[\text{Au}(\text{C}\equiv\text{CPh})_2]^-$  ( $2099\text{ cm}^{-1}$ )<sup>30</sup> and  $[\text{Bu}_4\text{N}]^+[\text{Au}(\text{C}\equiv\text{CPh})_2]^-$  ( $2098\text{ cm}^{-1}$ ),<sup>31</sup> in which the anion is not subjected to any specific influence of the large “innocent” phosphonium or ammonium cations. In contrast to the results in solution, in the solid state only the ionic form is present.

The same compound has also been obtained from several other reactions, including treatment of  $(\text{Me}_3\text{P})\text{Au}(\text{C}\equiv\text{CPh})_3$  with silver nitrate or  $(\text{AgC}\equiv\text{CPh})_n$  in dichloromethane, indicating selective transfer of ligands between the two metal cations. In all cases it was found to be advantageous if an excess of  $\text{Me}_3\text{P}$  was present in the reaction mixture.

To obtain information on the nature of the product generated in the absence of excess  $\text{Me}_3\text{P}$ , solutions of  $(\text{Me}_3\text{P})\text{Au}(\text{C}\equiv\text{CPh})$  and  $[(\text{Me}_3\text{P})_2\text{Ag}]^+[\text{Au}(\text{C}\equiv\text{CPh})_2]^-$  in dichloromethane were left at room temperature for some time before workup, allowing  $\text{Me}_3\text{P}$  and solvent vapors to escape. Subsequent workup afforded colorless and yellow crystals. The former were again identified as  $[(\text{Me}_3\text{P})_2\text{Ag}]^+[\text{Au}(\text{C}\equiv\text{CPh})_2]^-$ , while the latter (mp  $195\text{ }^\circ\text{C}$  with decomposition) were shown to have the *phosphine-deficient* composition  $[(\text{Me}_3\text{P})_2\text{Ag}_3\text{Au}_3(\text{C}\equiv\text{CPh})_6]$ . A crystal structure determination revealed the presence of  $[(\text{Me}_3\text{P})_2\text{Ag}]^+$  cations and  $[\text{Ag}_2\text{Au}_3(\text{C}\equiv\text{CPh})_6]^-$  anions associated into strings with an alternating sequence of ions.

In dichloromethane solution rapid ligand exchange is observed in NMR experiments, analogous to the behavior described for  $[(\text{Me}_3\text{P})_2\text{Ag}]^+[\text{Au}(\text{C}\equiv\text{CPh})_2]^-$ . In the IR spectrum of the solid (KBr) the  $\nu(\text{C}\equiv\text{C})$  band is only slightly shifted, to  $2079\text{ cm}^{-1}$ , as compared to the signal for the  $\text{Me}_3\text{P}$ -rich starting material ( $2097\text{ cm}^{-1}$ ), suggesting that the new environment of the  $[\text{Au}(\text{C}\equiv\text{CPh})_2]^-$  anions has only a marginal influence on the bonding in the phenylethynyl groups. The electronic absorption spectrum of the compound in dichloromethane solution at  $20\text{ }^\circ\text{C}$  is very similar to that of  $(\text{Me}_3\text{P})\text{Au}(\text{C}\equiv\text{CPh})$ , suggesting that the bands have to be assigned to intraligand transitions of the  $\text{Au}-\text{C}\equiv\text{CPh}$  units. Solutions cooled to  $77\text{ K}$  show yellow-green emission with a maximum at  $534\text{ nm}$ , not very different from the emission of the solid at  $556\text{ nm}$  (Figure 1). This result suggests that the cluster does not disintegrate in solution at low temperature.

## Structural Results

*Bis(trimethylphosphine)silver(I) bis(phenylethynyl)gold(I)* crystallizes in orthorhombic needles of space group *Pbcm* with four formula units in the unit cell. In the crystals, the components are disordered in equal distribution over two sets of atomic sites, which were found to account for all atoms except for the hydrogen atoms of two methyl groups (C102, C202). The two

(21) Schmidbaur, H.; Schier, A. *Sci. Synth.* **2004**, 691.

(22) Schmidbaur, H. *Organogold Compounds*; Slawisch, A., Ed.; Springer-Verlag: Berlin, 1980.

(23) Fackler, J. P., Jr.; Liu, C. W. *Sci. Synth.* **2004**, 663.

(24) Gimeno, M. C.; Laguna, A. In *Comprehensive Coordination Chemistry II*; McCleverty, J. A., Meyer, T. J., Eds.; Elsevier: Oxford, U.K., 2004; p 911.

(25) Wei, Q.-H.; Zhang, L.-Y.; Yin, G.-Q.; Shi, L.-X.; Chen, Z.-N. *J. Am. Chem. Soc.* **2004**, *126*, 9940.

(26) Vicente, J.; Chicote, M.-T.; Alvarez-Falcon, M. M. *Organometallics* **2005**, *24*, 4666.

(27) Schuster, O.; Liau, R.-Y.; Schier, A.; Schmidbaur, H. *Inorg. Chim. Acta* **2005**, *358*, 1429.

(28) Glaser, C. *Liebigs Ann. Chem.* **1870**, *154*, 137.

(29) Corfield, P. W. R.; Shearer, H. M. M. *Acta Crystallogr., Sect. C: Cryst. Struct. Commun.* **1966**, *4*, 502.

(30) Schuster, O.; Schmidbaur, H. *Organometallics* **2005**, *24*, 2289.

(31) Schuster, O.; Schmidbaur, H. *Inorg. Chim. Acta*, in press.

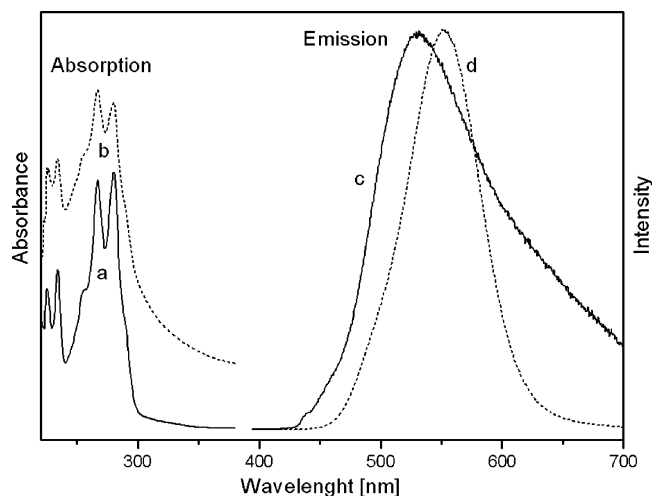


**Figure 1.** Absorption spectra of (a)  $(\text{Me}_3\text{P})\text{Au}(\text{C}\equiv\text{CPh})$  and (b)  $[(\text{Me}_3\text{P})_2\text{Ag}_3\text{Au}_3(\text{C}\equiv\text{CPh})_6]$  in  $\text{CH}_2\text{Cl}_2$  at room temperature and emission spectra of  $[(\text{Me}_3\text{P})_2\text{Ag}_3\text{Au}_3(\text{C}\equiv\text{CPh})_6]$  (c) in solution ( $\text{CH}_2\text{Cl}_2$ ,  $\lambda_{\text{exc}}$  390 nm) and (d) in the solid state ( $\lambda_{\text{exc}}$  400 nm) at room temperature.

$\text{Me}_3\text{P}$  ligands at the silver atom are not related by symmetry, but their conformation approaches quite closely the point group  $D_{3d}$ . The Ag–P distances of 2.419(5) and 2.368(5) Å (average 2.393 Å) are longer than the Au–P distances in  $[(\text{Me}_3\text{P})_2\text{Au}]^+$  cations (e.g. 2.304(6) Å for the cation of  $[(\text{Me}_3\text{P})_2\text{Au}]^+\text{Cl}^-$ ), as expected on the basis of new data on atomic radii.<sup>32,33</sup>

The axis P1–Ag1–P2 is approximately linear (angle 175.8(2) Å). Each cation is attached to two anions through Ag–Au metallophilic bonding with distances Au1–Ag1 = 3.206(2) Å and Ag1–Au1' = 3.224(2) Å. The resulting chain of alternating Ag and Au atoms is quasi-linear, with angles Au1–Ag1–Au1' and Ag1–Au1–Ag1' both at 179.53(4)° (Figure 2).

In the anions, the angle C11–Au1–C21 is 176.3(9)° with distances Au1–C11 = 1.99(2) Å and Au1–C21 = 2.02(2) Å. The two phenyl rings within each anion are roughly coplanar. Each C11–Au1–C21 axis is tilted against the two neighboring P1–Ag1–P2 axes by 69° (average). The Ag–Au–Ag–Au chains run parallel to the *a* axis of the unit cell. The projection shown in Figure 3 suggests that the tilting of the axes of the cations away from the axes of the anions is due to crystal packing. Note that the structure of the heterobimetallic  $[(\text{Me}_3\text{P})_2\text{Ag}]^+[\text{Au}(\text{C}\equiv\text{CPh})_2]^-$  differs severely from that of the homobimetallic analogue  $[(\text{Me}_3\text{P})_2\text{Ag}]^+[\text{Ag}(\text{C}\equiv\text{CPh})_2]^-$  with its strongly bent cations and anions.<sup>29</sup>

*[Bis(trimethylphosphine)silver(I)(+)]{bis[μ<sup>3</sup>-silver(I)]tris[μ<sup>2</sup>,η<sup>2</sup>:η<sup>2</sup>-bis(phenylethynyl)gold(I)](-)}* forms yellow monoclinic crystals of space group *Cc* with four formula units in the unit cell. The cations have conformations different from those in the precursor salt  $[(\text{Me}_3\text{P})_2\text{Ag}]^+[\text{Au}(\text{C}\equiv\text{CPh})_2]^-$ , with their symmetry approaching quite closely point group  $D_{3h}$  (instead of  $D_{3d}$ ). The angle P1–Ag1–P2 is 177.1(1)°, and the torsional angle C11–P1–P2–C21 is 5.6°, with the Ag–P bonds equidistant at 2.392(3) Å.

The pentanuclear anion ( $\text{Ag}_2\text{Au}_3$ ) can be described in various approaches. Its idealized symmetry is  $D_{3h}$ , with the gold atoms of three collinear  $\text{PhC}\equiv\text{CAuC}\equiv\text{CPh}$  anions forming an equilateral triangle. The two silver cations are inserted into this anion triple on the 3-fold axis and on the levels of the triple bonds to

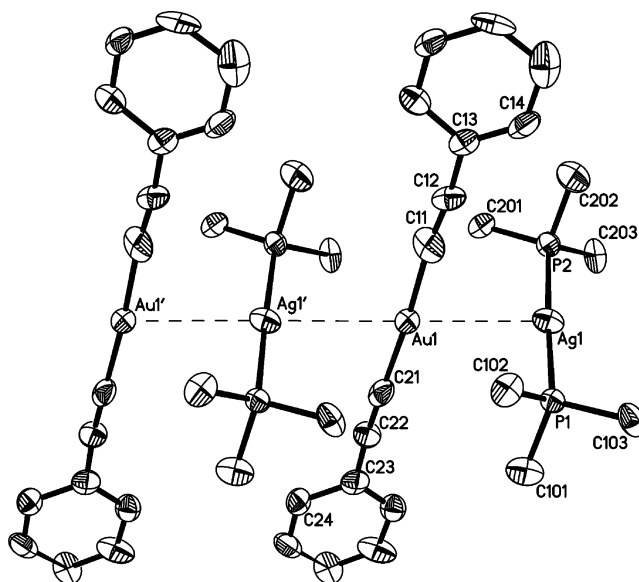


**Figure 2.** Chain of alternating cations and anions in the crystal structure of  $[(\text{Me}_3\text{P})_2\text{Ag}]^+[\text{Au}(\text{C}\equiv\text{CPh})_2]^-$  forming a linear axis of metal atoms connected by metallophilic bonding (ORTEP, 50% probability ellipsoids, hydrogen atoms omitted). Selected bond lengths (Å) and angles (deg): Ag1–P1 = 2.419(5), Ag1–P2 = 2.368(5), Au1–C11 = 1.99(2), Au1–C21 = 2.02(2), C11–C12 = 1.27(3), C21–C22 = 1.16(3); P1–Ag1–P2 = 175.8(2), C11–Au1–C21 = 176.3(9), Ag1–Au1–Ag1' = 179.53(4), Au1–Ag1–Au1' = 179.53(4).

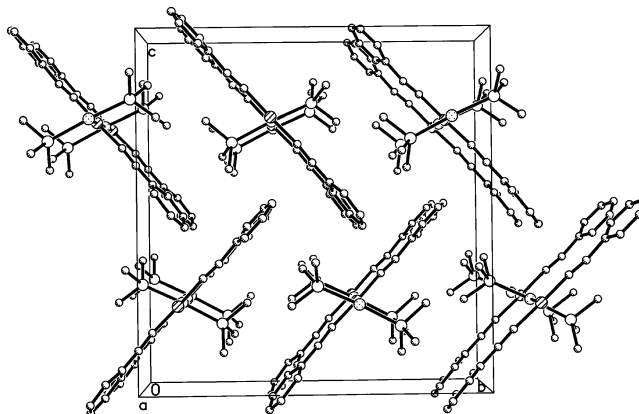


**Figure 3.** Packing of the chains shown in Figure 2 in the unit cell of  $[(\text{Me}_3\text{P})_2\text{Ag}]^+[\text{Au}(\text{C}\equiv\text{CPh})_2]^-$  projected parallel to the chain of metal atoms along the *a* axis (arbitrary radii for all atoms).

allow for interactions with six carbon atoms for each of them (Figure 4). In these positions, the silver atoms are also in close contact with the gold atoms, with distances ranging from 2.854(2) to 3.0390(9) Å, which clearly represent metallophilic bonding. The metal core  $\text{Ag}_2\text{Au}_3$  thus has a trigonal-bipyramidal structure with six axial–equatorial Ag–Au bonds, but with the equatorial–equatorial Au–Au contacts (3.95 Å average) too long for significant metallophilic contributions.

The structure type of the pentanuclear anion is known from previous work by Abu-Salah,<sup>17–20</sup> who prepared and characterized several species  $[\text{M}_2\text{M}'_3(\text{C}\equiv\text{CR})_6]^-$  featuring various combinations of M, M' = Cu, Ag, Au, with  $[\text{mBu}_4\text{N}]^+$  or  $[(\text{Ph}_3\text{P})_2\text{N}]^+$  counterions. The present case is special in that the anionic cluster is associated with the  $[(\text{Me}_3\text{P})_2\text{Ag}]^+$  cation into chains of alternating cationic and anionic components, which are linked through Ag–Au metallophilic bonding. Two of the three gold atoms of the anion entertain such Ag–Au contacts, while the

(32) Bayler, A.; Schier, A.; Bowmaker, G. A.; Schmidbaur, H. *J. Am. Chem. Soc.* **1996**, *118*, 7006.

(33) Tripathi, U. M.; Bauer, A.; Schmidbaur, H. *J. Chem. Soc., Dalton Trans.* **1997**, 2865.



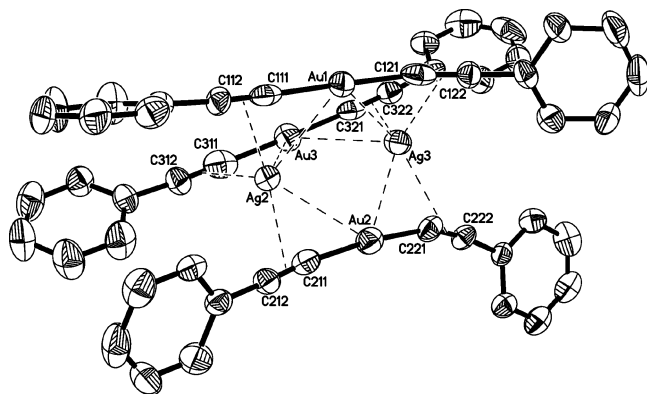


**Figure 4.** Structure of the anion in crystals of  $[(\text{Me}_3\text{P})_2\text{Ag}]^+[\text{Ag}_2\text{Au}_3(\text{C}\equiv\text{CPh})_6]^-$ . (ORTEP, 50% probability ellipsoids, hydrogen atoms omitted). Selected bond lengths ( $\text{\AA}$ ) and angles (deg): Au1–C111 = 1.99(3), Au1–C121 = 2.00(2), Au2–C211 = 2.02(2), Au2–C221 = 2.01(1), Au3–C311 = 2.01(2), Au3–C321 = 1.99(1), C111–C112 = 1.22(2), C121–C122 = 1.25(2), C211–C212 = 1.23(2), C221–C222 = 1.21(2), C311–C312 = 1.20(2), C321–C322 = 1.23(2); C111–Au1–C121 = 174.3(5), C211–Au2–C221 = 173.8(5), C311–Au1–C321 = 178.5(5). For intermetallic distances, see Figure 5.

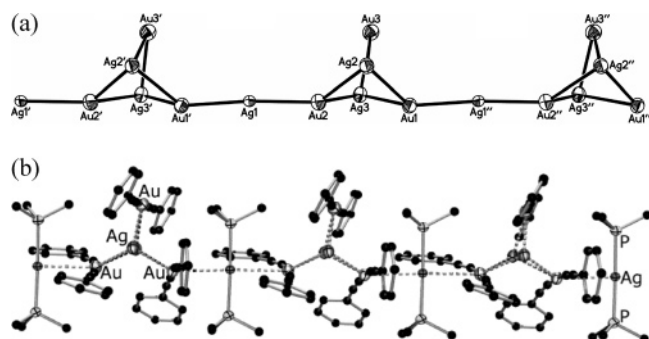


**Figure 5.** Aggregation of cations and anions of the compound  $[(\text{Me}_3\text{P})_2\text{Ag}]^+[\text{Ag}_2\text{Au}_3(\text{C}\equiv\text{CPh})_6]^-$  into chains: (a) core unit of metal atoms (ORTEP); (b) chain including the ligands (arbitrary radii, hydrogen atoms omitted). Selected bond lengths ( $\text{\AA}$ ) and angles (deg): Ag1–P1 = 2.392(3), Ag1–P2 = 2.392(3), Au1–Ag1' = 2.9996(8), Au1–Ag2 = 2.9397(9), Au1–Ag3 = 3.0390(9), Au2–Ag1 = 2.9945(8), Au2–Ag2 = 2.9676(9), Au2–Ag3 = 2.854(2), Au3–Ag2 = 3.001(1), Au3–Ag3 = 3.004(1); P1–Ag1–P2 = 177.1(1), Au1'–Ag1–Au2 = 171.26(3), Au1–Ag2–Au2 = 85.10(3), Au1–Ag2–Au3 = 79.99(2), Au2–Ag2–Au3 = 85.29(3), Au1–Ag3–Au2 = 85.31(3), Au1–Ag3–Au3 = 78.39(3), Au2–Ag3–Au3 = 87.23(3).

third one (Au3) is not involved (Figure 5). The distances Ag1–Au2 and Ag1–Au1' of 2.9945(8) and 2.9996(8)  $\text{\AA}$ , respectively, are short and very similar to the *intraanionic* interactions, suggesting rather strong *interionic* linkages.

### Computational Studies

From the preceding discussion, it is clear that, besides the metallophilic interactions, electrostatic interactions play an important role in the extended structures characterized. Metallophilic interactions are mainly of dispersive character<sup>34</sup> and thus are not amenable to a quantitative description by density functional methods based on current (semi-) local exchange-correlation potentials.<sup>35</sup> We therefore focused our computational

(34) Pyykkö, P. *Chem. Rev.* **1997**, *97*, 597.

(35) Koch, W.; Holthausen, M. C. *A Chemist's Guide to Density Functional Theory*, 2nd ed.; Wiley-VCH: Weinheim, Germany, 2002; Sect. 12.4.

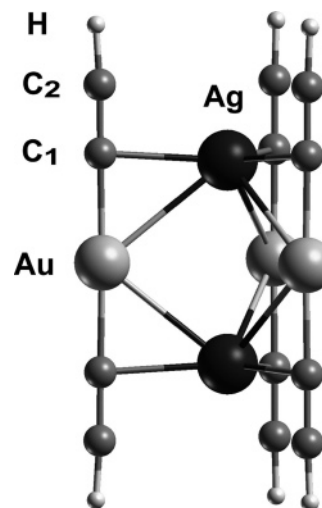


**Figure 6.** Optimized structure of the model cluster  $[\text{Ag}_2\text{Au}_3(\text{C}\equiv\text{CH})_6]^-$ . (The atomic numbering is different from that used in the crystallographic part.)

**Table 1.** Crystal Data and Data Collection and Structure Refinement Details

|   | $[(\text{Me}_3\text{P})_2\text{Ag}]^+[\text{Ag}(\text{C}\equiv\text{CPh})_2]^-$ | $[(\text{Me}_3\text{P})_2\text{Ag}]^+[\text{Ag}_2\text{Au}_3(\text{C}\equiv\text{CPh})_6]^-$ |
|---|---|--|
| empirical formula                                       | $\text{C}_{22}\text{H}_{22}\text{AgAuP}_2$                                      | $\text{C}_{54}\text{H}_{48}\text{Ag}_3\text{Au}_3\text{P}_2$                                 |
| $M_r$   | 653.17  | 1673.37  |
| cryst syst  | orthorhombic  | monoclinic   |
| space group   | <i>Pbcm</i>   | <i>Cc</i>  |
| $a/\text{\AA}$  | 6.4292 (2)  | 33.0696 (4)  |
| $b/\text{\AA}$  | 18.6655 (4)   | 9.9668 (2)   |
| $c/\text{\AA}$  | 19.2969 (5)   | 18.6939 (3)  |
| $\alpha/\text{deg}$                                     | 90  | 90   |
| $\beta/\text{deg}$                                      | 90  | 123.9803(6)  |
| $\gamma/\text{deg}$                                     | 90  | 90   |
| $V/\text{\AA}^3$  | 2315.71(11)   | 5109.27(15)  |
| $\rho_{\text{calcd}}/\text{g cm}^{-3}$                  | 1.873   | 2.175  |
| $Z$   | 4   | 4  |
| $F(000)$  | 1240  | 3120   |
| $\mu(\text{Mo K}\alpha)$ ( $\text{cm}^{-1}$ )           | 73.15   | 98.06  |
| $T/\text{K}$  | 143   | 143  |
| no. of rflns measd                                      | 56 468  | 67 806   |
| no. of unique rflns                                     | 2161 ( $R_{\text{int}} = 0.054$ )   | 59 586 ( $R_{\text{int}} = 0.075$ )  |
| no. of refined params/restraints                        | 229/0   | 565/2  |
| $R1$ ( $I \geq 2\sigma(I)$ )                            | 0.0523  | 0.0371   |
| $wR2^a$   | 0.1061  | 0.0959   |
| Flack parameter   |   | 0.080(5)   |
| weighting scheme  |   |  |
| $a$   | 0.0000  | 0.0470   |
| $b$   | 36.4130   | 31.3640  |
| $\sigma_{\text{fin}}(\text{max/min})/e \text{\AA}^{-3}$ | 0.967/–1.210  | 2.295/–2.518   |

<sup>a</sup>  $wR2 = \{\sum[w(F_o^2 - F_c^2)^2]/\sum[w(F_o^2)^2]\}^{1/2}$ ;  $w = 1/[\sigma^2(F_o^2) + (ap)^2 + bp]$ ,  $p = (F_o^2 + 2F_c^2)/3$ .

efforts toward elucidating the structure and bonding in the anionic cluster complex  $[\text{Ag}_2\text{Au}_3(\text{C}\equiv\text{CPh})_6]^-$ . To this end, we carried out model calculations applying a scalar-relativistic density functional approach. We modeled this complex as an isolated moiety in idealized  $D_{3h}$  symmetry. Also, we replaced the phenylethynyl by ethynyl ligands to simplify the calculations (Figure 6).

As a check of our model strategy, we compare in Table 2 pertinent bond lengths of  $[\text{Au}(\text{C}\equiv\text{CR})_2]^-$  for R = H, CH<sub>3</sub> to the crystal structure<sup>30</sup> of  $[\text{Bu}_4\text{N}]^+[\text{Au}(\text{C}\equiv\text{CPh})_2]^-$ . The largest deviation, 0.004  $\text{\AA}$ , between diethynylgold and dipropynylgold anions is found for the Au–C bond lengths, supporting ethynylide as the model ligand. Deviations from the experimental data for the bis(phenylethynyl)gold anion are somewhat

**Table 2. Pertinent Structure Parameters<sup>a</sup> of the Moiety [Au(C≡CR)<sub>2</sub>]<sup>-</sup> from Calculation and Experiment**

|                                    | R              |                              |                 |
|------------------------------------|----------------|------------------------------|-----------------|
|                                    | H <sup>b</sup> | CH <sub>3</sub> <sup>b</sup> | Ph <sup>c</sup> |
| Au–C <sub>1</sub>                  | 1.953          | 1.957                        | 1.992           |
| C <sub>1</sub> –C <sub>2</sub>     | 1.227          | 1.228                        | 1.205           |
| C <sub>1</sub> '–Au–C <sub>1</sub> | 180            | 180                          | 175             |

<sup>a</sup> Bond lengths are given in Å and angles in deg. <sup>b</sup> Calculation, this work. <sup>c</sup> Experiment, [<sup>n</sup>Bu<sub>4</sub>N]<sup>+</sup>[Au(C≡CPh)<sub>2</sub>]<sup>-</sup>.<sup>28</sup>

**Table 3. Pertinent Structure Parameters Calculated for the Model Complex [Ag<sub>2</sub>Au<sub>3</sub>(C≡CH)<sub>6</sub>]<sup>-</sup> and Related Models<sup>a</sup> Including Point Charges (PC) in Comparison with Averaged Experimental Results for [Ag<sub>2</sub>Au<sub>3</sub>(C≡CPh)<sub>6</sub>]<sup>-</sup>**

| system <sup>b</sup>                | [Ag <sub>2</sub> Au <sub>3</sub> L <sub>6</sub> ] <sup>-</sup> | [Ag <sub>2</sub> Au <sub>3</sub> L <sub>6</sub> ]PC <sub>3</sub> | [PC <sub>2</sub> Au <sub>3</sub> L <sub>6</sub> ] <sup>-</sup> | exptl <sup>c</sup> |
|------------------------------------|--|--|--|--------------------|
| Au–Au                              | 3.912  | 3.950  | 2.888  | 3.952              |
| Au–Ag                              | 2.904  | 2.946  | 2.472  | 2.968              |
| Au–C <sub>1</sub>                  | 1.960  | 1.957  | 1.962  | 1.998              |
| Ag–C <sub>1</sub>                  | 2.295  | 2.304  | 1.841  | 2.353              |
| C <sub>1</sub> –C <sub>2</sub>     | 1.229  | 1.229  | 1.223  | 1.223              |
| C <sub>1</sub> '–Au–C <sub>1</sub> | 178  | 179  | 170  | 176                |

<sup>a</sup> For details of computational models see text. Bond lengths are given in Å and angles in deg. <sup>b</sup> L = C≡CH. <sup>c</sup> Reference 28.

larger. The Au–C distance calculated for the diethynylgold anion is ~0.04 Å shorter while the C≡C bond is ~0.02 Å longer than the corresponding experimental values. These deviations are not easily attributed to a single source; they may mainly reflect deviations due to crystal-packing effects. Such packing effects are obviously responsible for the angle C–Au–C': calculated at 180° for the isolated anion but determined to be 175° in the crystal structure (Table 2). The calculated C≡C bond length of 1.23 Å in the ethynyl ligands of [Au(C≡CH)<sub>2</sub>]<sup>-</sup> falls between the corresponding values calculated for an isolated ethynyl radical (1.21 Å) and an ethynylide anion (1.25 Å). Potential derived charges<sup>36</sup> confirm this situation to be intermediate between ionic and covalent. They amount to 0.23 e for Au and -0.62 e for the C≡CH ligands of [Au(C≡CH)<sub>2</sub>]<sup>-</sup>. The metal–ligand bond of this moiety is mainly due to  $\sigma$  bonding between Au(d<sub>z<sup>2</sup></sub>) and  $\sigma$  orbitals of the ligands. In fact, a three-orbital interaction between the d<sub>z<sup>2</sup></sub> and s orbitals of Au and the symmetric linear combination of the  $\sigma$  frontier orbitals of the two ligands occurs, leading to a high-lying nonbonding sd hybrid orbital on Au (HOMO-1). The  $\pi$  system of the ethynyl ligands forms the HOMO of the anion [Au(C≡CH)<sub>2</sub>]<sup>-</sup>, with some Au(d) contribution, and the HOMO-2.

Optimization of the isolated anion [Ag<sub>2</sub>Au<sub>3</sub>(C≡CH)<sub>6</sub>]<sup>-</sup> yields a structure which closely agrees with experimental findings for [Ag<sub>2</sub>Au<sub>3</sub>(C≡CPh)<sub>6</sub>]<sup>-</sup>, averaged according to the approximate D<sub>3h</sub> symmetry (Table 3). As for the isolated moiety [Au(C≡CH)<sub>2</sub>]<sup>-</sup>, the Au–C distance of 1.96 Å is ~0.04 Å shorter than the experimental value. The C≡C bond is calculated at 1.23 Å, slightly longer (0.01 Å) than found in experiment, just as obtained for the diethynylgold anion. Comparing experimental results, one notes that the average value of C≡C bonds in the crystal structure of the cluster anion [Ag<sub>2</sub>Au<sub>3</sub>(C≡CPh)<sub>6</sub>]<sup>-</sup> is 0.02 Å longer than for the single anion<sup>30</sup> [Au(C≡CPh)<sub>2</sub>]<sup>-</sup>, while our calculations yield identical values for diethynylgold and the cluster anion (Tables 2 and 3). In the crystal structure, C≡C bond lengths scatter by the same amount (0.02 Å), which is comparable to the experimental uncertainty (see the Supporting Information); thus, experimental and calculated results are compatible. Our computational models also result in metal–

metal distances that are somewhat shorter than those obtained in the crystal structure analysis: Au–Au distances are 0.04 Å shorter and Au–Ag distances 0.07 Å shorter than the corresponding values in the crystal structure. The distance between Ag atoms and the ethynyl ligands, as measured by the distance Ag–C<sub>1</sub>, compare reasonably well with experiment: 2.30 Å. Calculated distances Ag–C<sub>1</sub> are 0.05 Å shorter than the experimental values. In the cluster compound, the [Au(C≡CH)<sub>2</sub>]<sup>-</sup> units stay almost linear; the angle C<sub>1</sub>–Au–C<sub>1</sub>' is calculated to be bent 2° from the main axis of the cluster.

One may advance two major arguments to rationalize the general tendency of the model calculations of underestimating interatomic bond distances, leaving aside the limited accuracy of the computational methods applied. One expects crystal-packing effects to elongate interatomic distances due to steric stress; on the other hand, the crystal field of the surrounding ions, missing in the model calculations, also may influence the geometry. To inspect qualitatively this latter effect, we considered a neutral model of D<sub>3h</sub> symmetry where we placed three point charges of 1/3 e in the plane of the Au triangle at radial distances of 2.997 Å from the Au atoms (model [Ag<sub>2</sub>(AuL)<sub>3</sub>]PC<sub>3</sub>, Table 3); that distance is the average of Au–Ag distances involving Ag atoms of nearest-neighbor counterions in the crystal structure. As the charge of the cluster ion [Ag<sub>2</sub>Au<sub>3</sub>(C≡CH)<sub>6</sub>]<sup>-</sup> is neutralized in this complex, it may serve as a rough qualitative model to probe crystal field effects.

Indeed, the largest changes resulting in this model in comparison to the isolated cluster ion are elongations of metal–metal distances. The Au–Au distance increases by 0.04 Å to 3.95 Å; this exact reproduction of the experimental average is likely due to fortuitous error compensation. The Au–Ag contacts are also elongated by 0.04 Å to 2.95 Å, now also in very satisfactory accord with experiment (2.97 Å). All other pertinent structure characteristics are hardly altered: bond distances change by less than 0.01 Å, and the angle C<sub>1</sub>–Au–C<sub>1</sub>' changes by about 1°.

All metal centers of the cluster ion [Ag<sub>2</sub>Au<sub>3</sub>(C≡CPh)<sub>6</sub>]<sup>-</sup> exhibit formal oxidation state +I. For the Au atoms, this is qualitatively confirmed by the results calculated for our model compound [Ag<sub>2</sub>Au<sub>3</sub>(C≡CH)<sub>6</sub>]<sup>-</sup>, as revealed by inspecting the C≡C bond lengths. As for [Au(C≡CH)<sub>2</sub>]<sup>-</sup>, the calculated C–C distance of 1.23 Å (Table 3) indicates a partially ionic character of the Au–ethynylide bond (see above). To probe the character of metal–metal interactions and, in particular, the oxidation state of the Ag atoms in the model compounds, we invoked a third model system, [PC<sub>2</sub>(AuL)<sub>3</sub>]<sup>-</sup>, where we replaced the Ag atoms of the cluster by point charges of 1 e (Table 3). We optimized the structure of this model, keeping the point charges at fixed locations to represent the effect of the crystal environment. As the main result, we determined a very large reduction of the Au–Au distances, by about 1 Å. Surprisingly, this strong “contraction” of the complex has only a marginal effect on other structural parameters. The Au–C<sub>1</sub> bonds increase by 0.002 Å, and the C≡C bonds contract by 0.006 Å. The bending of diethynylgold units, as measured by the angle C<sub>1</sub>–Au–C<sub>1</sub>', increases from 2 to 10°. We observe hardly any geometry relaxation when the Ag atoms are replaced by point charges. This finding suggests marginal orbital interactions between silver and diethynylgold units and thus points to a strongly ionic nature of the Ag centers as well as to a mainly ionic interaction between these Ag(I) ions and diethynylgold units. A possible covalent interaction of the Ag centers with the ethynyl  $\pi$  systems has to be classified as weak, as the C≡C bond lengths elongate only slightly (by 0.002 Å) in the presence of Ag ions. Potential-

(36) Besler, B. H.; Merz, K. M.; Kollman, P. A. *J. Comput. Chem.* **1990**, *11*, 431.

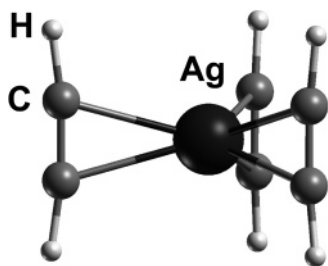


**Figure 7.** Optimized structure of the model complex  $[\text{Ag}(\text{HC}\equiv\text{CH})_3]^+$ .

**Table 4. Characteristics of the Complex  $[\text{Ag}(\text{HC}\equiv\text{CH})_3]^+$  Calculated with Different Constraints and Approximations (Models 1–4)<sup>a</sup>**

|                      | C <sub>1</sub> –C <sub>2</sub> | Ag–C <sub>1</sub> | C <sub>1</sub> –C <sub>1</sub> ' | C <sub>2</sub> –C <sub>1</sub> –Ag | BE   |
|----------------------|--------------------------------|-------------------|----------------------------------|------------------------------------|------|
| model 1 <sup>b</sup> | 1.217                          | 2.385             | 3.994                            | 75                                 | 25.0 |
| model 2 <sup>c</sup> | 1.217                          | 2.370             | 3.967                            | 75                                 | 24.8 |
| model 3 <sup>d</sup> | 1.216                          | 2.295             | 3.967                            | 93                                 | 23.5 |
| model 4 <sup>e</sup> | 1.216                          | 2.295             | 3.967                            | 93                                 | 19.4 |

<sup>a</sup> Bond lengths are given in Å, angles in deg, and binding energies per HC≡CH ligand (BE) in kcal/mol. <sup>b</sup> Geometry optimized in  $D_{3h}$  symmetry. <sup>c</sup> As for model 1, but C–C' fixed at the value 3.967 Å calculated for the complex  $[\text{Ag}_2\text{Au}_3(\text{C}\equiv\text{CH})_6]^-$ . <sup>d</sup> As for model 2, but symmetry constraints reduced to  $C_{3v}$  and height of Ag fixed as calculated for the complex  $[\text{Ag}_2\text{Au}_3(\text{C}\equiv\text{CH})_6]^-$  (Ag–C = 2.295 Å). <sup>e</sup> As for model 3 (including geometry), but Ag cations replaced by point charge of 1 e.

derived charges of the cluster ion  $[\text{Ag}_2\text{Au}_3(\text{C}\equiv\text{CH})_6]^-$ , which probe the long-range electrostatic field,<sup>36</sup> confirm our geometry-based analysis. While Ag centers are assigned a charge of 0.51 e, Au centers are characterized by only 0.14 e, while the ethynyl ligands carry a charge of 0.41 e, in line with the intermediate bond length of the ethynyl ligands between radicals and anions and with the molecular orbital analysis of the  $[\text{Au}(\text{C}\equiv\text{CH})_2]^-$  moieties described above.

To quantify the interaction in the cluster compounds between the cationic Ag centers and the ethynyl  $\pi$  systems, we examined a series of models of the complex  $[\text{Ag}(\text{HC}\equiv\text{CH})_3]^+$  (Figure 7). In comparison to the cluster compound  $[\text{Ag}_2\text{Au}_3(\text{C}\equiv\text{CH})_6]^-$  this complex allows for an easier inspection of effects of  $\pi$  orbital interactions of Ag; in addition, an energy analysis of this interaction is possible, which is hampered by the strong ionic contributions in the gold–silver cluster. First, we optimized this complex in  $D_{3h}$  symmetry (model 1), allowing optimal bonding to the acetylene  $\pi$  orbitals. In model 2, we fixed the C–C distances between different acetylene ligands at 3.967 Å, which corresponds to the C<sub>1</sub>–C<sub>1</sub>' distance in  $[\text{Ag}_2\text{Au}_3(\text{C}\equiv\text{CH})_6]^-$ , to account for the proper size of the cluster compound. In a third step toward the structure of  $[\text{Ag}_2\text{Au}_3(\text{C}\equiv\text{CH})_6]^-$ , we lowered the symmetry of our model complex to  $C_{3v}$  and shifted the Ag ion from the plane defined by the centers of the C≡C bonds to the position obtained by optimizing  $[\text{Ag}_2\text{Au}_3(\text{C}\equiv\text{CH})_6]^-$ , to yield Ag–C<sub>1</sub> distances identical with those in the latter cluster. This model, model 3, mimics the structural characteristics of  $[\text{Ag}_2\text{Au}_3(\text{C}\equiv\text{CH})_6]^-$ , but the diethynylgold ligands are replaced by acetylene. In a last step (model 4), we substituted a point charge of 1 e for the silver cation, without further relaxation of the geometry.

The optimized structure of  $[\text{Ag}(\text{HC}\equiv\text{CH})_3]^+$  in the  $D_{3h}$  symmetry (model 1) yields an Ag–C distance of 2.39 Å (Table 4), about 0.1 Å longer than the value for Ag–C<sub>1</sub> in the cluster  $[\text{Ag}_2\text{Au}_3(\text{C}\equiv\text{CH})_6]^-$ . The diameter of the complex, as judged by the distance C–C' of 3.99 Å between corresponding C atoms of different acetylene ligands, is very similar to the value calculated for C<sub>1</sub>–C<sub>1</sub>' in  $[\text{Ag}_2\text{Au}_3(\text{C}\equiv\text{CH})_6]^-$  (3.97 Å). Thus,

we conclude that the ethynyl groups in the cluster compound have a distance close to optimal for an interaction between Ag and the  $\pi$  systems of the ethynyl ligands. With 1.22 Å, the C≡C bonds of the ligands are shorter than in the cluster compound, reflecting the formally neutral nature of these ligands compared to their more anionic character in the diethynylgold moieties.

In model 1, the binding energy per acetylene ligand is calculated at 25 kcal/mol. Due to the similar diameters of the two complexes compared, model 2 yields almost the same ligand binding energy (Table 4). Stronger effects have been determined for model 3, where the Ag cation is shifted from the plane through the centers of the C≡C bonds to a plane defined by the three corresponding C atoms of the ligands. Then the Ag–C distance shrinks from 2.39 to 2.30 Å for the closer C atoms. Interestingly, the shift of the Ag cations has only a negligible effect on the length of the C≡C bond (Table 4). Also the binding energy of the ligands decreases by only 1.5 kcal/mol compared to that in model 1. Replacing the Ag cation in model 3 by a point charge of 1 e results in a further slight decrease of the binding energy per ligand to about 19 kcal/mol. This last result corroborates that most of the binding between the acetylene ligands and the Ag<sup>+</sup> centers is due to electrostatic effects. In model 3, only about 15% of this interaction (4 kcal/mol per ligand) can be ascribed to orbital interactions.

In summary, in agreement with our analysis of the properties of the cluster  $[\text{Ag}_2\text{Au}_3(\text{C}\equiv\text{CH})_6]^-$ , our model study of  $[\text{Ag}(\text{HC}\equiv\text{CH})_3]^+$  points toward a mainly electrostatic interaction. If anything, orbital interactions play only a minor role. In view of the closed-shell d<sup>10</sup> electronic structure of Ag<sup>+</sup> these results appear plausible.

## Conclusions

In the present account a particularly striking example is presented of the self-assembly of bis(phenylethynyl)gold(I) anions with silver cations to produce the pentanuclear mixed-metal aggregate  $[\text{Ag}_2(\text{PhC}\equiv\text{CAu}\equiv\text{CPh})_3]^-$  with an  $\text{Ag}_2\text{Au}_3$  core of  $D_{3h}$  symmetry (Figure 5): in dichloromethane solutions containing  $[\text{PhC}\equiv\text{CAu}\equiv\text{CPh}]^-$  anions,  $[(\text{Me}_3\text{P})_2\text{Ag}]^+$  cations are stripped of their tertiary phosphine ligands and the bare Ag<sup>+</sup> cations are trapped between three rodlike bis(phenylethynyl)gold anions. The compound  $[(\text{Me}_3\text{P})_2\text{Ag}]^+[\text{Au}(\text{C}\equiv\text{CPh})_2]^-$ , therefore, is only stable in the presence of excess trimethylphosphine, which counteracts the dissociation of the cation. Otherwise, loss of Me<sub>3</sub>P is observed in both solution and the solid state. With excess Me<sub>3</sub>P present in the mother liquor, colorless  $[(\text{Me}_3\text{P})_2\text{Ag}]^+[\text{Au}(\text{C}\equiv\text{CPh})_2]^-$  can be crystallized. In the crystals, the cations and anions are associated to chains with alternating components through mixed-metal metallophilic bonding along linear –Ag–Au–Ag–Au– axes (Figure 2). In the absence of Me<sub>3</sub>P, from the same solutions yellow crystals of  $[(\text{Me}_3\text{P})_2\text{Ag}]^+[\text{Ag}_2\text{Au}_3(\text{C}\equiv\text{CPh})_6]^-$  are obtained. This compound is strongly photoluminescent as a solid and in solution at room temperature (Figure 1). The absorption and emission profiles are very similar, suggesting undissociated clusters in solution. In the crystal, the cluster anions are associated with the cations via Ag–Au metallophilic bonding in which only two of the three equatorial gold atoms of the  $\text{Ag}_2\text{Au}_3$  bipyramid are involved (Figures 5 and 6).

Complexes of the type  $[\text{M}'_2\text{M}'_3(\text{C}\equiv\text{CR})_6]^-$  have been obtained previously with various combinations of coinage metals M/M', including  $[\text{Cu}_2\text{Au}_3(\text{C}\equiv\text{CPh})_6]^-$ , for which the unusual structure has first been determined.<sup>17,20</sup> The structural details of known examples are not very different, except for distances depending on the change in ionic radii of the coinage metals.



To shed light on the nature of bonding in these clusters, density functional calculations of the model complex  $[\text{Ag}_2\text{Au}_3(\text{C}\equiv\text{CH})_6]^-$ , imposing  $D_{3h}$  symmetry constraints, have been carried out, which resulted in satisfactory agreement with suitably averaged experimental structure data for  $[\text{Ag}_2\text{Au}_3(\text{C}\equiv\text{CPh})_6]^-$ . Deviations could partially be traced to the packing of the ions in the crystal and to effects of the resulting electrostatic field. Comparison with a model where  $\text{Ag}^+$  ions are replaced by positive point charges as well as structural and energetic analyses of the model complex  $[\text{Ag}(\text{HC}\equiv\text{CH})_3]^+$  have pointed toward a mainly ionic binding situation within the cluster ions  $[\text{Ag}_2\text{Au}_3(\text{C}\equiv\text{CH})_6]^-$ , between the building blocks  $\text{Ag}^+$  and  $[\text{Au}(\text{C}\equiv\text{CH})_2]^-$ .

## Experimental Section

**General Procedure.** All organometallic syntheses were performed in a dry deoxygenated dinitrogen atmosphere using standard Schlenk techniques. All solvents were distilled from an appropriate drying agent and stored over molecular sieves (4 Å) and under nitrogen. Solutions were handled at  $-78^\circ\text{C}$  unless otherwise stated and protected against light. All standard chemicals were purchased from Aldrich or Fluka and used without further purification.  $[\text{Ag}(\text{C}\equiv\text{CPh})_n]^-$  and  $(\text{Me}_3\text{P})\text{Au}(\text{C}\equiv\text{CPh})^{27}$  were prepared as described in the literature. Mass spectra were recorded on a Finnigan MAT 90 spectrometer using FAB as an ionization method. NMR spectra were obtained at various temperatures on JEOL-400 and JEOL-270 spectrometers. Chemical shifts are reported in  $\delta$  values relative to the residual solvent resonances converted to TMS ( $^1\text{H}$ ).  $^{31}\text{P}\{^1\text{H}\}$  NMR spectra are referenced to external aqueous  $\text{H}_3\text{PO}_4$  (85%). The single-crystal X-ray diffraction measurements were performed at  $-130^\circ\text{C}$  on a Nonius DIP 2020 diffractometer using graphite-monochromated Mo K $\alpha$  radiation.

**(Phenylethynyl)(trimethylphosphine)silver(I),  $(\text{Me}_3\text{P})\text{AgC}\equiv\text{CPh}$ .** To a stirred suspension of 418 mg of  $[\text{Ag}(\text{C}\equiv\text{CPh})_n]$  (2.0 mmol) in 40 mL of  $\text{CH}_2\text{Cl}_2$  was added 2.0 mmol of  $\text{PMe}_3$  dissolved in 2 mL of toluene. The resulting clear solution was protected against light and stirred for  $1/2$  h before the solvents were removed in vacuo. Recrystallization from dichloromethane/pentane at  $-30^\circ\text{C}$  gave 485 mg (85% yield) of a colorless solid. Mp:  $173^\circ\text{C}$  dec.  $^1\text{H}$  NMR ( $\text{CD}_2\text{Cl}_2$ , room temperature):  $\delta$  1.22 (d,  $^2J_{\text{HP}} = 9.5$  Hz, 9H,  $\text{P}(\text{CH}_3)_3$ ), 7.26–7.47 (m, 5 H,  $\text{C}_6\text{H}_5$ ).  $^{13}\text{C}\{^1\text{H}\}$  NMR ( $\text{CD}_2\text{Cl}_2$ , room temperature):  $\delta$  15.5 (d,  $^1J_{\text{CP}} = 17.7$  Hz,  $\text{P}(\text{CH}_3)_3$ ), 102.9 (s,  $\text{Ag}-\text{C}\equiv\text{CPh}$ ), 118.8 (s,  $\text{Ag}-\text{C}\equiv\text{CPh}$ ), 124.0 (s,  $i-\text{C}_6\text{H}_5$ ), 127.8 (s,  $p-\text{C}_6\text{H}_5$ ), 128.1 (s,  $o-\text{C}_6\text{H}_5$ ), 132.1 (s,  $m-\text{C}_6\text{H}_5$ ).  $^{31}\text{P}\{^1\text{H}\}$  NMR ( $\text{CD}_2\text{Cl}_2$ , room temperature):  $\delta$   $-38.7$  (s,  $\text{P}(\text{CH}_3)_3$ ). Anal. Calcd for  $\text{C}_{11}\text{H}_{14}\text{AgP}$  (285.07): C, 46.35; H, 4.95. Found: C, 45.88; H, 4.80.

**[Bis(trimethylphosphine)silver(I)][bis(phenylethynyl)aurate(I)],  $[(\text{Me}_3\text{P})_2\text{Ag}][\text{Au}(\text{C}\equiv\text{CPh})_2]$ .** A sample of  $(\text{Me}_3\text{P})\text{Ag}(\text{C}\equiv\text{CPh})$  (29 mg, 0.1 mmol) was dissolved in 20 mL of  $\text{CH}_2\text{Cl}_2$ , and 1 equiv of  $(\text{Me}_3\text{P})\text{Au}(\text{C}\equiv\text{CPh})$  (37 mg, 0.1 mmol) was added. Stirring was continued for 10 min at room temperature. After addition of 0.5 mL of  $\text{PMe}_3$  (0.5 mmol, 1.0 M in toluene), pentane was diffused slowly into the clear reaction mixture at  $-30^\circ\text{C}$ . A total of 57 mg (87% yield) of colorless needles was collected. Mp:  $153\text{--}155^\circ\text{C}$  dec. IR (KBr,  $\text{cm}^{-1}$ ): 2097 (m,  $\nu(\text{C}\equiv\text{C})$ ). MS (FABpos,  $m/z$ ): 615 (40.2%)  $[(\text{PhC}\equiv\text{C})_2\text{Ag}_2\text{Au}]^+$ , 481 (21.1%)  $[(\text{PhC}_2)\text{AgAu}(\text{PMe}_3)]^+$ , 349 (100%)  $[(\text{Me}_3\text{P})_2\text{Au}]^+$ , 317 (93.3%)  $[(\text{PhC}\equiv\text{C})\text{Ag}_2]^+$ , 273 (20.1%)  $[(\text{Me}_3\text{P})\text{Au}]^+$ , 261 (34.5%)  $[(\text{Me}_3\text{P})_2\text{Ag}]^+$ , 185 (45.8%)  $[(\text{Me}_3\text{P})\text{Ag}]^+$ . MS (FABneg,  $m/z$ ): 399 (18.1%)  $[(\text{PhC}\equiv\text{C})_2\text{Au}]^-$ , 153 (100%)  $[(\text{MeP})\text{Ag}]^-$ . Anal. Calcd for  $\text{C}_{22}\text{H}_{28}\text{AgAuP}_2$  (659.17): C, 40.19; H, 4.28. Found: C, 40.33; H, 4.35.

**[Bis(trimethylphosphine)silver(I)][hexakis( $\mu_2,\eta^2$ -phenylethynyl)trigold(I)disilver(I)],  $[(\text{Me}_3\text{P})_2\text{Ag}][\text{Ag}_2\text{Au}_3(\text{C}\equiv\text{CPh})_6]$ .** The reaction was carried out as described above, using  $(\text{Me}_3\text{P})\text{Ag}(\text{C}\equiv\text{CPh})$  (29 mg, 0.1 mmol) and  $(\text{Me}_3\text{P})\text{Au}(\text{C}\equiv\text{CPh})$  (37 mg, 0.1 mmol) in 20 mL of  $\text{CH}_2\text{Cl}_2$ , but no  $\text{PMe}_3$  was added before crystallization. Colorless needles and yellow plates were obtained. Washing the product mixture with three 1 mL portions of  $\text{CH}_2\text{Cl}_2$  yielded 30 mg (54% yield) of yellow plates. Mp:  $195\text{--}196^\circ\text{C}$  dec. IR (KBr,  $\text{cm}^{-1}$ ): 2079 (m,  $\nu(\text{C}\equiv\text{C})$ ). MS (FABpos,  $m/z$ ): 615 (64.0%)  $[(\text{PhC}\equiv\text{C})_2\text{Ag}_2\text{Au}]^+$ , 481 (37.0%)  $[(\text{PhC}\equiv\text{C})\text{AgAu}(\text{PMe}_3)]^+$ , 349 (100%)  $[(\text{Me}_3\text{P})_2\text{Au}]^+$ . Anal. Calcd for  $\text{C}_{54}\text{H}_{48}\text{Ag}_3\text{Au}_3\text{P}_2$  (1673.37): C, 38.76; H, 2.89. Found: C, 39.19; H, 2.89.

**Crystal Structure Determinations.** The single crystals were placed in inert oil on the top of a glass pin and transferred to the cold gas stream of the diffractometer. Crystal data were collected using a Nonius DIP2020 system with monochromated Mo K $\alpha$  ( $\lambda = 0.71073$  Å) radiation at  $-130^\circ\text{C}$ . The structures were solved by direct methods (SHELXS-97) and refined by full-matrix least-squares calculations on  $F^2$  (SHELXL-97).<sup>37</sup> Non-hydrogen atoms were refined with anisotropic displacement parameters. Hydrogen atoms were placed in idealized positions and refined using a riding model with fixed isotropic contributions if possible. Crystals of  $[(\text{Me}_3\text{P})_2\text{Ag}][\text{Au}(\text{C}\equiv\text{CPh})_2]$  were found to be disordered (sof = 0.5). Due to this fact, hydrogen atoms of methyl groups on special positions (C102, C202) could be neither calculated nor found in the Fourier map. Residual peaks/holes in the electron density maps are all very close to the heavy-metal atoms. Further information on crystal data, data collection, and structure refinement is summarized in Table 1. Important interatomic distances and angles are given in the figure captions. Complete lists of displacement parameters and tables of interatomic distances and angles have been deposited with the Cambridge Crystallographic Data Centre, 12 Union Road, Cambridge CB2 1EZ, U.K.. The data are available on request on quoting CCDS files 292086 and 292087.

**Computational Section.** In calculations, we applied the all-electron LCGTO-FF-DF approach (linear combination of Gaussian-type orbitals fitting function density functional),<sup>38</sup> as implemented in the parallel program ParaGauss.<sup>39,40</sup> To account for relativistic effects, we chose the scalar-relativistic variant of the Douglas–Kroll–Hess approach to relativistic density functional theory.<sup>41</sup> Spin–orbit effects were neglected, because all heavy-element species examined have a closed-shell electronic structure. Structures have been optimized with an LDA exchange–correlation functional,<sup>42</sup> while energies were calculated self-consistently with a more accurate GGA functional,<sup>43,44</sup> employing LDA geometries. This strategy is motivated by the well-known tendency of GGA functionals to overestimate bond lengths of heavy-element compounds, whereas LDA functionals overestimate binding energies but yield accurate geometries.<sup>45,46</sup> To represent the Kohn–Sham

(37) Sheldrick, G. M., SHELXL-97: Programs for Crystal Structure Analysis; University of Göttingen, Göttingen, Germany, 1997.

(38) Dunlap, B. I.; Rösch, N. *Adv. Quantum Chem.* **1990**, *21*, 317.

(39) Belling, T.; Grauschopf, T.; Krüger, S.; Mayer, M.; Nörtemann, F.; Stauffer, M.; Zenger, C.; Rösch, N. In *High Performance Scientific and Engineering Computing*; Bungartz, H.-J., Durst, F., Zenger, C., Eds.; Lecture Notes in Computational Science and Engineering 8; Springer: Heidelberg, Germany, 1999; pp 439–453.

(40) Belling, T.; Grauschopf, T.; Krüger, S.; Nörtemann, F.; Stauffer, M.; Mayer, M.; Nasluzov, V. A.; Birkenheuer, U.; Hu, A.; Matveev, A. V.; Fuchs-Rohr, M. S. K.; Shor, A. M.; Neyman, K. M.; Ganyushin, D. I.; Kercharoen, T.; Woiterski, A.; Gordienko, A. B.; Majumder, S.; Rösch, N. ParaGauss Version 3.0; Technische Universität München, München, Germany, 2004.

(41) Rösch, N.; Krüger, S.; Mayer, M.; Nasluzov, V. A. In *Recent Developments and Applications of Modern Density Functional Theory*; Seminario, J., Ed.; Theoretical and Computational Chemistry Series 4, Elsevier: Amsterdam, 1996; p 497.

(42) Vosko, S. H.; Wilk, L.; Nusair, M. *Can. J. Phys.* **1980**, *58*, 1200–1211.

(43) Becke, A. D. *Phys. Rev. A* **1988**, *38*, 3098–3100.

(44) Perdew, J. P. *Phys. Rev. B* **1986**, *33*, 8822–8824; **1986**, *34*, 7406.

(45) Ziegler, T. *Chem. Rev.* **1991**, *91*, 651–667.

(46) Görling, A.; Trickey, S. B.; Gisdakis, P.; Rösch, N. In *Topics in Organometallic Chemistry*; Brown, J., Hoffmann, P., Eds.; Springer: Heidelberg, Germany, 1999; Vol. 4, pp 9–165.

orbitals, we used very flexible Gaussian-type basis sets, contracted in generalized fashion. For Au, a set of 21s, 17p, 11d, and 7f exponents was contracted to [11s, 10p, 7d, 3f].<sup>47</sup> The basis set for Ag was (18s, 13p, 9d) contracted to [7s, 6p, 4d].<sup>48</sup> For C and H, we used standard basis sets of sizes (9s, 5p, 1d)/[5s, 4p, 1d] and (6s, 1p)/[4s, 1p], respectively.<sup>49</sup> The auxiliary basis set, used in the LCGTO-FF-DF approach to represent the electronic charge density when evaluating the Hartree contribution, was constructed according to a standard procedure.<sup>38</sup> The atomic basis sets were augmented by sets of five p-type polarization exponents on all atoms, five d-type exponents on all centers but H, and five f-type exponents on the metal centers. Each set of these "polarization" exponents was constructed as a geometric series with a progression of 2.5, starting with 0.1, 0.2, and 0.3 au for p, d, and f types, respectively.

(47) Häberlen, O. D.; Rösch, N. *Chem. Phys. Lett.* **1992**, *199*, 491.

(48) Matveev, A. V.; Neyman, K. M.; Yudanov, I. V., Rösch, N. *Surf. Sci.* **1999**, *426*, 123.

**Acknowledgment.** This work was supported by the Deutsche Forschungsgemeinschaft, Fonds der Chemischen Industrie, Volkswagenstiftung, and Heraeus GmbH.

**Supporting Information Available:** CIF files giving details of crystal data, data collection and structure refinement details, atomic coordinates, isotropic and anisotropic thermal parameters, and all bond lengths and angles. This material is available free of charge via the Internet at <http://pubs.acs.org>.

OM050985Z

(49) (a) Van Duijneveldt, F. B. *IBM Res. Rep.* **1971**, RJ 945. (b) Huzinaga, S.; Andzelm, J.; Klobukowski, M.; Radzio-Andzelm, E.; Sakai, Y.; Tatewaki, H. *Gaussian Basis Sets for Molecular Calculations*; Elsevier: Amsterdam, 1984 (C: d exponent 0.60). (c) Frisch, M. J.; Pople, J. A.; Binkley, J. S. *J. Chem. Phys.* **1984**, *80*, 3265 (H: p exponent 1.0).